CHAPTER 6

CRESTED PORCUPINE OPTIMIZER FOR INTELLIGENT ESTIMATION OF CURRENT RIPPLE IN POWER FACTOR CORRECTION INTERLEAVED BOOST CONVERTERS FOR ELECTRIC VEHICLE CHARGING

Ankarao Mogili[1], D. Vijayalakshmi[2] , A.Thanikasalam[3] V. Velmurugan[4]

[1*] Department of Electrical and Electronics Engineering, JNTUA College of Engineering, Andhra Pradesh 515002, India.

ankaraomogili@gmail.com

[2] Department of Physics, School of Basic Sciences, Vels Institute of Science Technology and Advanced Studies

Chennai, Tamil Nadu 600117, India. **vijayalakshmi.sbs@vistas.ac.in** &

viji.duraikannu@gmail.com

[3] Department of Marine Engineering, Academy of Maritime Education and Training (AMET) Deemed to be University, Chennai, Tamil Nadu 603112, India.

thanikasalama@ametuniv.ac.in

[4] Department of Mechanical and Automation Engineering, Sri Sairam Engineering College, Chennai, Tamil Nadu 600044, India. **velmurugan.mu@sairam.edu.in**

Abstract

Enhancing efficiency and power quality (PQ) in electric vehicle (EV) charging systems depends on power factor correction (PFC) interleaved boost converters (IBC). Traditional methods to assess current ripple produce misleading results which leads to decreased system performance and increased power losses. This research presents the Crested Porcupine Optimizer (CPO) as a novel solution for intelligent current ripple estimation in electric vehicle charging systems to overcome existing method limitations. The main goal consists of minimizing ripple formation while also reducing Total Harmonic Distortions (THD). The Proportional-Integral (PI) controller gain parameter optimization occurs through CPO processing which raises the converter performance standards. The proposed solution implemented on MATLAB while evaluated performance with Artificial Neural Network (ANN) and Bald Eagle Search Optimization (BESO) and Long Short-Term Memory (LSTM). Results show the CPO approach delivers THD at 0.99% which supports effective harmonic suppression to enhance PQ for EV chargers. The evaluation demonstrates that CPO successfully enhances the current ripple estimation capability to improve PFC IBC system operations in EV charging applications.

Keywords— Crested Porcupine Optimizer, Electric Vehicle Charging, Interleaved Boost Converter, Power Factor Correction, and Total Harmonic Distortion.

I. INTRODUCTION

(A) BACKGROUND

The ability to achieve improved performance as well as reduced input current ripple in EV charging systems depends solely on IBC operations [1]. Multiple parallel working phases constitute the fundamental operational method in these converters to produce better current distribution while suppressing high-frequency oscillations that affect both PQ quality and grid stability [2]. Determining the present ripple in these systems proves demanding because both non-linear switching dynamics and integrating electromagnetic interference (EMI) respond to changing load conditions [3]. Standard estimation methods need simplified models because researchers must create advanced analytical methods to properly identify system changes effectively. Artificial intelligence (AI)-based methods with machine learning (ML) and deep learning models act as robust estimation tools in order to determine current ripple levels for PFC IBC systems [4]. The evaluation methods achieve successful measurements of complex electrical waveforms through their analysis of nonlinear dynamic interactions. The implementation of AI enhances estimation systems to deliver exceptional reliability performance alongside optimal power efficiency as well as vital predictive maintenance capabilities [5]. Integrated intelligent power monitoring methods for vehicle charging systems deliver reliable PQ conversion in addition to extending power component durability and system lifespan.

(b) Challenges

Many barriers prevent accurate current ripple assessment in PFC IBC systems because of the intricate relationships between various system parameters and switching characteristics and external electromagnetic disturbances. Non-linear behavior occurs in the system because duty cycle variations together with parasitic elements and component tolerances affect expected ripple patterns. Current ripple measurement during high-frequency switching becomes inaccurate because of EMI and noise so signal processing methods with advanced filtering have become necessary for accurate results. Standard analysis techniques apply basic premises that restrict their capability to track system dynamics and operational adaptations .Another significant challenge is the requirement for fast and adaptive estimation techniques that can operate efficiently under varying load conditions and grid fluctuations. ML and AI-based approaches, while promising; require extensive training data, computational resources, and robust feature extraction methods to achieve high accuracy.

Furthermore, implementing AI-driven solutions in practical power electronics applications requires adaptability and seamless integration with existing control algorithms without introducing excessive latency. Ensuring the reliability, scalability, and robustness of intelligent estimation techniques remains a critical hurdle in advancing PFC IBC technology for EV charging applications.

(c) Literature Survey

Several research studies have focused on IBC for EV Charging, utilizing different techniques and approaches. A review of some of these works is provided below,

According to F. Aslay and N. S. Ting [6], an ANN model was created to estimate the output current ripple of a PFC AC/DC IBC used in EV battery chargers based on changes in load, switching frequency, and inductance current ripple. Additionally, the enhanced ANN model was contrasted with a few other ML methods. P. Mane and R. M. Linus have demonstrated the need to enhance the power efficiency of photovoltaic (PV) grid-connected inverters for EV rapid charging applications [7]. The system includes a High-Gain Interleaved dubbed SEPIC-Cuk (HGISC), a BESO-ANFIS algorithm, and Voltage-Oriented Control (VOC) for the PV inverter. The HGIBC converter enhances power efficiency, and VOC with proportional resonance ensures the best possible energy transfer to the grid. BESO-ANFIS MPPT, which was newly introduced, was used to dynamically track the PV array's MPP under different conditions. The bidirectional battery converter within the energy storage system optimized power consumption. EV charging applications require a decreased sensor based bridgeless boost (BLB) PFC converter which feeds a full-bridge inductor-inductor capacitor (FBLLC) converter according to R. Pandey and B. Singh [8]. The first component of the PFC-BLB converter operated its boost inductors under continuous conduction mode. The BLB converter uses pulse width modulated control for switching at a predetermined frequency yet the FBLLC converter enables CC/CV battery EV charging through pulse frequency modulation control.

N. C. Szekely et al. [9] introduced a PFC application based on the newly developed power stage architecture known as IDBIC.The newly introduced PFC rectifier was innovative because of its combined characteristics, which included high voltage gain, interleaved operation at the input, and the ability to produce three distinct output voltage levels. A single-phase bridge rectifier, an AC input L-C-L filter, an IDBIC power stage, a group of output capacitors, and a set of variable high-power rheostats acting as a DC load comprise the hardware utilized in this application.

Highlighting the benefits and drawbacks of the new power stage topology within the framework of a contemporary and environmentally friendly AC to DC conversion solution was the primary goal of the undertaken study. S. Kaushik et al. [10] have provided a workable solution to address these problems. Using load torque and defined driving cycles, like the Urban Dynamometer Driving Schedule, the power demand of hybrid EVs (HEVs) was evaluated. First, the implementation of the LSTM based on multistep velocity predictors utilizing a warm-up approach was made simpler by feature extraction approaches, which enhance the extraction of significant characteristics from historical driving cycle data. The HEV system receives this anticipated future velocity profile as input. Second, a modified interleaved DC-DC boost converter was connected to the battery of the HEV system.

(d) Research Gap and Motivation

A significant research gap exists in the integration and optimization of power performance in EV charging systems, particularly in enhancing the interaction between PFC techniques, converter topologies, and energy management algorithms. While advancements like ANN models for estimating current ripple in PFC AC/DC inverters and BESO-ANFIS for dynamic MPPT in PV systems have been explored, there is a lack of comprehensive studies combining these methods for efficient power management in grid-connected inverters. Furthermore, current solutions, such as interleaved converters and HVDC systems for energy storage in EV chargers, fail to fully address scalability under variable load conditions, optimal energy transfer to the grid, and seamless integration of multiple renewable energy sources. Additionally, existing techniques like ANN, BESO, and LSTM models present drawbacks that hinder their broader application. ANN models, while effective in pattern recognition, are prone to overfitting and lack transparency. BESO, despite its optimization capabilities, can be computationally expensive and may not always converge to a global optimum in complex, dynamic environments. The aforementioned limitations are motivated to do this work.

(e) Contribution

The following is a summary of the main contributions of this manuscript:

- The study proposes the use of the CPO for intelligent estimation of current ripple in PFCIBC for EV charging, providing a novel optimization approach.
- The CPO technique is utilized to optimize the gain parameter of the PI controller, resulting in improved PFC and minimized ripple in the converter system.

- The use of CPO leads to a reduction in THD, demonstrating the approach's ability to enhance PQ in EV charging systems through harmonic suppression.
- A comprehensive comparison is made between the proposed CPO method and other existing techniques, such as ANN, BESO, and LSTM, highlighting the effectiveness of CPO in optimizing current ripple.
- The proposed CPO-based method is implemented on the MATLAB platform, confirming its potential for optimizing PFC and current ripple estimation in EV charging systems.

(f) Novelty

The main contribution of this work introduces the CPO method to perform intelligent current ripple estimation in PFC IBC for EV charging systems. The implemented CPO approach succeeds where conventional methods fail because it optimizes PI controller gain parameters for minimization of ripple and THD reduction. The PFC performance receives enhancement as well as EV charging PQ improvements through this approach. The results from comparing optimization techniques support CPO as the optimal solution for this application.

(g) Organization

The paper's remaining section is arranged as below: Part 2 shows the configuration of current ripple in PFC IBC for EV charging. Part 3 illustrates the proposed CPO Technique. Part 4 describes the results and discussion. Part 5 concludes the manuscript.

II. CONFIGURATION OFCURRENT RIPPLE IN PFC INTERLEAVED BOOST CONVERTERS FOR EV CHARGING

Figure 1 illustrates an EV charging system integrating a PV source with an IBC topology. The PV system supplies power through an isolated DC-DC converter, which is connected to a DC bus. The DC bus is also linked to a DC-AC IBC that interfaces with the EV. A PI controller governs the system’s operation, ensuring optimal power regulation and minimizing current ripple. The controller is further optimized using the proposed CPO technique, enhancing the system's efficiency and stability.

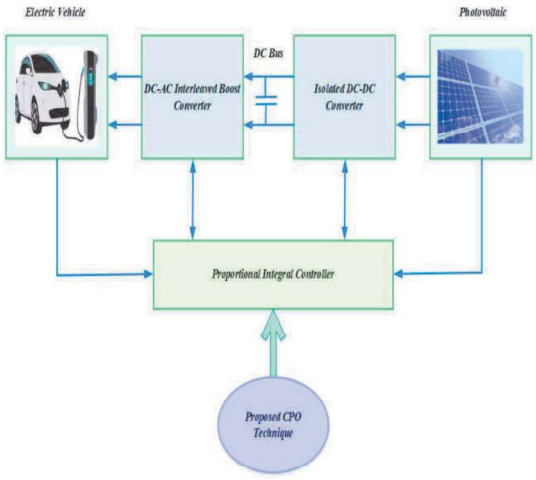

Figure 1: Structure ofI BC for EV Charging

A. Modelling of Electric Vehicle

The modelling of EVs as mobile energy storage discussed in this section. DifferentSoC, time of arrival and departure or charging or discharging, power and energy rating of the EVs must determine the charging or discharging routine. [11].

EVs' maximum charging and discharging rates are shown in Equation (1)-(2).

$$0 \le P_{a,t,\sigma}^{EV} \le \frac{P_{\max}^{Ev}}{\eta_c^{EV}} \forall t,\sigma \qquad (1).$$

$$0 \le P_{b,t,\sigma}^{EV} \le P_{\max}^{EV} \cdot \eta_d^{EV} \forall t,\sigma \qquad (2).$$

$P_{a,t}^{EV}$ and $P_{b,t}^{EV}$ indicates the EV charging and discharging at time t respectively.

Equation (3) and (4) are used to determine the EV's SoC.

$$H_{arrival}^{EV} = H_{start}^{EV} \qquad (3).$$

$$H_{departure}^{EV} = H_{end}^{EV} \qquad (4).$$

Here, H_{start}^{EV} and H_{end}^{EV} are the corresponding parameters for the EV starting and ending energy levels.

B. Modelling of Interleaved Boost Converter

There are 2 or more phases in the IBC stage. An inductor plus a low-side active switch make up each phase [12]. To lessen input current ripples and, consequently, the size of the input filters, a phase shift between the active switches is required. One way to show a phase shift between active switches is to

$$shift \geq \frac{360^{o}}{\phi} \quad (5).$$

where the number of interleaved phases is indicated by ϕ, a positive integer greater than or equal to 2.

$$d \geq \frac{\phi - 1}{\phi} \quad (6).$$

The IBC stage lowers magnetic storage in addition to current ripples. The magnetic element is cut in half in the 2-phase scenario, assuming that the inductors share the input current evenly.

$$\frac{C_2}{C_1} = \frac{\frac{1}{2} l \left(\frac{i}{2}\right)^2 + \frac{1}{2} l \left(\frac{i}{2}\right)^2}{\frac{1}{2} l i^2} \times 100 = 50\% \quad (7).$$

The reduction for C_{ϕ} is expressed as M.

$$M(\%) = \left(1 - \frac{1}{\phi}\right) \times 100 \quad (8).$$

Equation (8) does not show a decrease in the magnetic volume. Rather, the volume reduction should be compared as follows:

$$\partial = \frac{Vol_{k=1} - Vol_{k=\phi}}{Vol_{k=1}} \times 100 \quad (9).$$

where $Vol_{k=1}$ is the magnetic element's volume in a single-phase converter and $Vol_{k=\phi}$ is the magnetic element's volume in a multiphase converter with ϕ phases.

$$Pl_T = \frac{i_l^2 \times r_{dc}}{\phi} \quad (10).$$

$$Ps, co_T = \frac{i_{s,RMS}^2 \times r_{ON}}{\phi} \quad (11).$$

The duty cycle and the number of interleaved phases determine the input current ripples. The duty cycle parameters for additional phases during which ripple cancellation may take place are provided by

$$D_{\Delta e=0} = \left[\frac{1}{\phi}, \frac{2}{\phi}, ..., \frac{\phi - 1}{\phi}\right] \quad (12).$$

III. CRESTED PORCUPINE OPTIMIZER

The CPO is a nature-inspired optimization algorithm that mimics the behavior of porcupines in their natural habitat, particularly their method of self-protection and territorial behaviour [13]. It has gained attention for its ability to efficiently solve complex optimization problems by balancing exploration and exploitation. The general content of the CPO includes the definition of an initial population, fitness evaluation, and iterative updating of positions based on the behavior of porcupines. CPO is particularly advantageous due to its robust global search capabilities, fast convergence, and ability to avoid local minima, making it suitable for a wide range of applications, including those in power systems and EV charging optimization. It offers improved accuracy, reduced computation time, and better performance compared to many traditional optimization techniques, providing superior results in terms of PFC and harmonic suppression.The step by step process is described as follows,

Step 1: Initialization

The input parameters are set as the gain parameters of the PI controller.

Step 2: Random Generation

Following initialization, random vectors are used to create the input parameters at random.

$$E=\begin{bmatrix} E_1 \\ E_2 \\ \vdots \\ E_I \\ \vdots \\ E_n \end{bmatrix}=\begin{bmatrix} e_{1,1} & e_{1,2} & \cdots & e_{1,J} & \cdots & e_{1,D} \\ e_{2,1} & e_{2,2} & \cdots & e_{2,J} & \cdots & e_{2,D} \\ \vdots & \vdots & \vdots & \vdots & \vdots & \vdots \\ e_{I,1} & e_{I,2} & \cdots & e_{I,J} & \cdots & e_{I,D} \\ \vdots & \vdots & \vdots & \vdots & \vdots & \vdots \\ e_{n',1} & e_{n',2} & \cdots & e_{n',J} & \cdots & e_{n',D} \end{bmatrix} \quad (13).$$

where $e_{I,J}$ is the J[th] position of the I[th] response, D is the dimension size, and n' is the total number of viable solutions.

Step 3: Fitness Function

Fitness is assessed using the objective function.

$$F = Minimize\left(THD\right) \quad (14).$$

where F represents the fitness function.

Step 4: Exploration Stage

This stage displays the CPO's exploring mechanism. When a predator is far away, the CP uses one of 2 primary defensive strategies: the sight method or the sound strategy, depending on their defensive behaviour. These strategies involve surveying different regions to conduct a global exploration search.

The following section describes these strategies in detail and presents the mathematical formulas used to simulate them.

$$\vec{y}_I^{T+1} = \left(1 - \vec{V}_1\right) \times \vec{y}_I^{T} + \vec{V}_1 \times \left(\vec{x} + \sigma_3 \times \left(\vec{y}_{S1}^{T} - \vec{y}_{S2}^{T}\right)\right) \quad (15).$$

where S_1 *and* S_2 are 2 random integers within $[1, n]$, and randomly generated value between 0 and 1 is denoted as σ_3.

Step 5: Exploitation Stage

This stage involves the proposal of the CPO's exploitative mechanism. Depending on its protective behaviour, the CP uses either the odour strategy or the physical attack strategy as its 2 main defence mechanisms when a predator is in the area. These strategies focus on exploiting promising regions through a local search.

$$\vec{y}_I^{T+1} = \vec{y}_{cp}^{T} + \left(\alpha\left(1 - \sigma_4\right) + \sigma_4\right) \times \left(\delta \times \vec{y}_{cp}^{T} - \vec{y}_I^{T}\right) - \sigma_5 \times \delta \times \gamma_T \times \vec{f}_I^{T} \quad (16).$$

where σ_4 denotes a random number, $\vec{f}_I^{T}$ is the average force, α is a convergence speed factor, and $\vec{y}_I^{T}$ is theI^{th} individual's position at iteration. It also reflects the position's predator and the best-obtained solution.

Step 6: Termination Criteria

Examine the termination criteria. If the optimal solution has been attained, conclude the procedure. Otherwise, move on to step 3.

IV. RESULT AND DISCUSSION

This section evaluates the effectiveness of the CPO technique based on simulation results. This method is implemented on the MATLAB platform and tested against other existing approaches including ANN, LSTM, and BESO.

Figure 2 shows the analysis of the power factor as a function of load variation, ranging from 50% to 100%. The power factor remains consistently high, with values close to 1 across the entire range. At 50% load, the power factor is approximately 0.99 and remains stable up to 90% load. At 100% load, the power factor slightly improves to reach a value of 1. This indicates an efficient design of the PFC circuit, maintaining near-unity power factor regardless of load variation. Figure 3 presents the analysis of current ripple with respect to line voltage variation from 180 V to 260 V. At 180 V, the current ripple starts at approximately 1 A and decreases slightly to about 0.9 A at 200 V. It reaches its minimum value of around 0.6 A at 220 V. Beyond this point, the current ripple begins to increase, reaching approximately 1 A at 240 V and peaking at 1.3 A at 260 V.

This trend indicates that the current ripple varies nonlinearly with line voltage, with a noticeable dip near 220 V, suggesting an optimal operating point for reduced ripple.

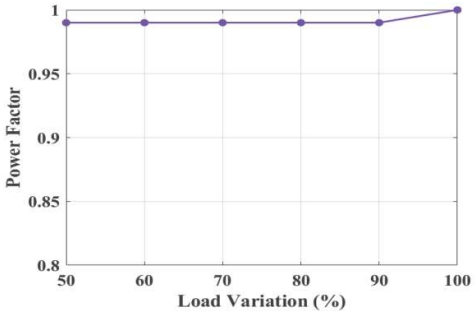

Figure 2:Analysis of Power Factor

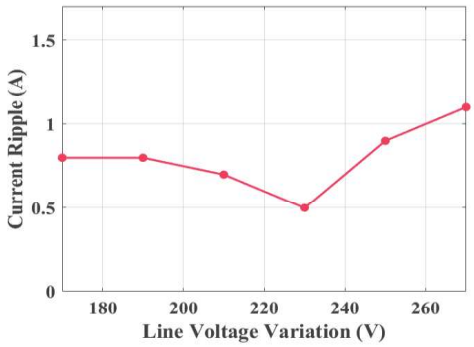

Figure 3: Analysis of Current Ripple

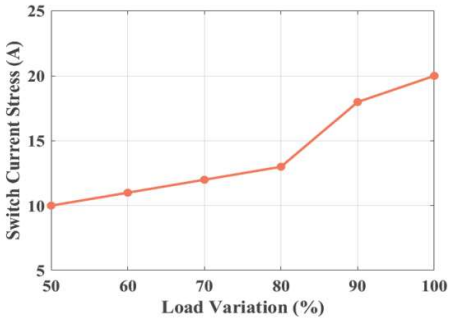

Figure 4: Analysis of Switch Current Stress

Figure 4 illustrates the variation in switch current stress as a function of load variation (%). At 50% load, the switch current stress is approximately 10 A. As the load increases to 60% and 70%, the stress rises slightly but remains below 15 A. At 80% load, the stress is around 15 A, indicating a gradual increase.

However, a sharp rise is observed beyond 80%, with the current stress exceeding 17 A at 90% load and reaching nearly 20 A at full load (100%).

This trend highlights the increasing stress on the switch as the load increases, with a more pronounced rise at higher loads.

TABLE 1: COMPARISON OF THD WITH PROPOSED AND EXISTING METHODS

Methods	THD (%)
ANN	3.61
LSTM	4.28
BESO	2.52
CPO (proposed)	0.99

Table 1 presents a comparative analysis of THD achieved using different techniques. The ANN method results in a THD of 3.61%, while the LSTM approach exhibits a higher THD of 4.28%. The BESO improves performance, reducing THD to 2.52%. The proposed CPO significantly outperforms all existing methods, achieving the lowest THD of 0.99%, indicating superior harmonic suppression and improved PQ in EV charging applications.

A. Discussion

This study investigates the intelligent estimation of current ripple in PFCIBC for EV charging, employing the CPO. The analysis reveals that the power factor remains near unity across varying load conditions, demonstrating the efficiency of the PFC system. Current ripple varies nonlinearly with line voltage, with a distinct reduction observed at around 220 V, indicating an optimal point for minimizing ripple. Higher load levels increase switch current stress and indicate a requirement for improved stress management strategies after reaching 80% load. The CPO proves most effective in harmonic suppression among all techniques because it produces the lowest THD and leads to substantial PV quality improvements for EV charging systems.

V. CONCLUSION

The research establishes that the CPO demonstrates proficient current ripple prediction capabilities when applied to PFC IBC in EV charging systems. The proposed method achieves successful THD reduction to 0.99% through optimal PI controller gain optimization which minimizes the ripple. CPO demonstrates remarkable superiority over ANN, BESO, and LSTM techniques when it comes to opTimizing current ripple and boosting PFC performance.

Overall, the proposed approach offers a promising solution for improving efficiency, reducing losses, and enhancing the reliability of EV charging systems. A limitation of this work is that the proposed CPO-based method was only tested in a simulation environment and not on physical hardware for real-time validation.

Future work could focus on implementing the optimization technique on physical EV charging systems to validate its performance in real-time applications.

REFERENCES

[1] O. Turksoy, U. Yilmaz, and A. Teke, "Efficient AC-DC power factor corrected boost converter design for battery charger in electric vehicles," Energy, vol. 221, p. 119765, 2021. DOI: 10.1016/j.energy.2021.119765.

[2] G. Jothimani, Y. Palanichamy, S. K. Natarajan, and T. Rameshkumar, "Single-phase front-end modified interleaved Luo power factor correction converter for on-board electric vehicle charger," Int. J. Circuit Theory Appl., vol. 49, no. 9, pp. 2655–2669, 2021. DOI: 10.1002/cta.3017.

[3] N. Ramadevi, R. Senthilkumar, and C. R. Balamurugan, "A novel bald eagle search optimised ANFIS controlled high gain sepic converter-based efficient regenerative charging control for electric vehicles," Electr. Eng., vol. •••, pp. 1–26, 2024. DOI: 10.1007/s00202-024-02603-5.

[4] Y. L. Lee, C. H. Lin, S. D. Lu, and H. D. Liu, "A novel high-performance two poles and two zeros digital compensation control strategy for electric vehicle lithium battery charging systems," J. Energy Storage, vol. 52, p. 105024, 2022. DOI: 10.1016/j.est.2022.105024.

[5] B. Singh and R. Kushwaha, "Power factor preregulation in interleaved Luo converter-fed electric vehicle battery charger," IEEE Trans. Ind. Appl., vol. 57, no. 3, pp. 2870–2882, 2021. DOI: 10.1109/TIA.2021.3061964.

[6] F. Aslay and N. S. Ting, "Machine learning-based estimation of output current ripple in PFC-IBC used in battery charger of electrical vehicles: A comparison of LR, RF and ANN techniques," IEEE Access, vol. 10, pp. 50078–50086, 2022. DOI: 10.1109/ACCESS.2022.3174100.

[7] Mane, P., & M. Linus, R. (2024). Optimizing EV fast charging infrastructure: integrating high-gain interleaved converter with advanced MPPT. Smart Science, 1-25.

[8] Kavitha, D., Sharmila, B., Ramkumar, M. S., Sivaramkrishnan, M., & Brindha, M. (2024, November). A Retrospective of Solar-Powered Charging Stations and E-Vehicles. In 2024 8th International Conference on Electronics, Communication and Aerospace Technology (ICECA) (pp. 131-135). IEEE.

[9] R. Pandey and B. Singh, "A power factor corrected resonant EV charger using reduced sensor based bridgeless boost PFC converter," IEEE Trans. Ind. Appl., vol. 57, no. 6, pp. 6465–6474, 2021. DOI: 10.1109/TIA.2021.3106616.

[10] N. C. Szekely, S. I. Salcu, V. M. Suciu, L. N. Pintilie, G. I. Fasola, and P. D. Teodosescu, "Power Factor Correction Application Based on Independent Double-Boost Interleaved Converter (IDBIC)," Appl. Sci. (Basel), vol. 12, no. 14, p. 7209, 2022. DOI: 10.3390/app12147209.

[11] S. Kaushik, K. Rachananjali, and V. Nath, “A novel LSTM-based EMS and interleaved DC-DC boost converter topology for real-time driving conditions in HEVs,” Electr. Eng., vol. 106, no. 5, pp. 1–20, 2024. DOI: 10.1007/s00202-024-02259-1.

[12] F. H. Aghdam, M. W. Mudiyanselage, B. Mohammadi-Ivatloo, and M. Marzband, “Optimal scheduling of multi-energy type virtual energy storage system in reconfigurable distribution networks for congestion management,” Appl. Energy, vol. 333, p. 120569, 2023. DOI: 10.1016/j.apenergy.2022.120569.

[13] A. Alzahrani, M. Ferdowsi, and P. Shamsi, “A family of scalable non-isolated interleaved DC-DC boost converters with voltage multiplier cells,” IEEE Access, vol. 7, pp. 11707–11721, 2019. DOI: 10.1109/ACCESS.2019.2891625.

[14] M. Abdel-Basset, R. Mohamed, and M. Abouhawwash, “Crested Porcupine Optimizer: A new nature-inspired metaheuristic,” Knowl. Base. Syst., vol. 284, p. 111257, 2024. DOI: 10.1016/j.knosys.2023.111257.